

# Destabilization of Internal Kink Mode by Energetic Electrons on the HL-2A Tokamak

W. Chen, X.T. Ding, Yi. Liu, G.L. Yuan, Y.P. Zhang, Y.B. Dong, X.Y. Song, J. Zhou, X.M. Song, W. Deng, Q.W. Yang, X.R. Duan, Y. Liu, and HL-2A team.

Southwestern Institute of Physics, P.O.Box 432 Chengdu 610041, China

E-mail contact of main authors: chenw@swip.ac.cn, dingxt@swip.ac.cn

**Abstract**—Strong burst of the internal kink mode has been observed during ECRH on the HL-2A. It has been experimentally identified that the energetic electrons, which deviate from Maxwell velocity distribution, excite the mode, which was so called electron fishbone (e-fishbone). The energy distribution of the electrons is indirectly measured by a hard X-ray detector (CdTe) with the pulse height analysis (PHA). When the counts of the energetic electrons with 35-70keV increase to a higher level, the mode can be observed obviously. The e-fishbone can be excited during off-axis ECRH deposited both the high field side and low field side. The modes propagate toroidally parallel to the precession velocity of deeply trapped ions which is in the same direction as the plasma current (co-current) and poloidally parallel to the electron diamagnetic drift velocity. In order to further identify with e-fishbone mode, the resonance condition of wave-particle has been investigated. Comparing with experimental results, the calculation analyses show that the mode frequency is close to the precession frequency of the barely trapped electrons (BTEs) or the barely circulating electrons (BCEs) when the magnetic shear is very weak or negative.

## 1. Introduction

Fishbone instabilities are related to the physics of the burning plasma [1], so it is very important to study this kind of instability in tokamak plasma theoretically and experimentally. Ion fishbone instability has been investigated in many tokamaks with neutral beam injection (NBI) [2-4], but the kinetic effect of energetic electrons on internal kink mode is not clear up to now [5, 6]. The kinetic effect of the energetic electrons on the mode was observed firstly on DIII-D with both NBI and off-axis electron cyclotron current drive (ECCD) [5]. The excitation mechanism was put down to the resonance between the barely trapped energetic electrons and the internal kink mode. Trapped energetic ions and barely trapped energetic electrons can excite the fishbone instability together. The pure e-fishbone instabilities are observed in the HL-1M tokamak with off-axis electron cyclotron resonance heating (ECRH) when the cyclotron resonance location is placed just outside the  $q = 1$  surface on the HFS of the magnetic surface. The addition of low-hybrid wave (LHW) to ECRH significantly enhances the mode [6, 7]. The e-fishbone is also observed on the FTU tokamak with lower hybrid current drive (LHCD) only [8, 9]. More recently, the e-fishbone related with double kink mode has also been observed on Tore Supra with LHCD [10].

To understand the e-fishbone instabilities with different heating, two kinds of excitation mechanism have been proposed: One is the precession resonance with the BTEs [5, 11]. It is the drift reversal effect that makes it possible for the BTEs to resonate with the internal kink

mode. This kind of interpretation mainly is based on the well-known ion fishbone theory [12, 13]. The other is the resonance with the BCEs at the negative magnetic shear [9, 14]. However, these explanations have not been identified by experiments and are still ambiguous, so the further experiments need carry out.

In the present paper, the observation of e-fishbone on the HL-2A tokamak is reported with the emphasis on the relation between the mode and spectra of the energetic electrons. The results analyzed by wave-particle resonance condition are compared with the experiments.

## 2. Experimental conditions

HL-2A is a medium-sized tokamak with a double null closed divertor. The typical parameters of the present experiment: major radius  $R = 1.65\text{m}$ , minor radius  $a = 0.40\text{m}$ , plasma current  $I_p = 100\text{--}350\text{ kA}$ , toroidal magnetic field  $B_t = 1.0\text{--}2.5\text{ T}$ , line-averaged density  $\langle n_e \rangle = (1\text{--}4) \times 10^{13}\text{ cm}^{-3}$ , edge safety factor  $q_a = 3\text{--}5$ , and a plateau duration of 0.3-1.0s.

The ECRH system with four 68GHz/500kW/1S gyrotrons has been built up and successfully used on HL-2A. The range of ECRH power is  $P_{ECRH} = (0\text{--}2)\text{ MW}$ . The ECRH power with O-mode (selected harmonic number  $n = 1$ ) or X-mode ( $n = 2$ ) is injected from the LFS.

The evolution of internal kink mode is followed by a 100 channel soft X-ray multi-camera system (5 arrays, 20 channels for each array); the energy range of its detector is 1eV-10keV. Figure 1(a) shows the arrangement of the soft X-ray array. The spatial and temporal resolution of the system is 2.5 cm and  $10\ \mu\text{s}$ , respectively. Their view covers the entire plasma cross section; only those channels with sight lines passing through the plasma core are shown in this work because our attention is focused on the  $q = 1$  surface in the plasma core. The drift direction of internal kink mode can be derived from the local soft X-ray emissions reconstructed by a tomographic technique.

The energy spectrum of energetic electrons is indirectly measured by CdTe diagnostic system on HL-2A. The CdTe detector is placed outside of the vacuum vessel in order to obtain information of the hard X-ray emission. The hard X-ray spectrum is obtained using PHA. The range of hard X-ray spectrum is 10-200 keV divided into eight channels discretionarily. The temporal resolution of the system is 1ms, and the highest energy resolution is 1 keV.

## 3. Experimental results

The e-fishbone was observed in the signals from a soft X-ray array (A1) shown in FIG.1. FIG 1b shows the typical temporal evolution of the soft X-ray intensity during ECRH in shot 7982. The parameters of this shot are: plasma current  $I_p = 300\text{ kA}$ , toroidal field  $B_t = 2.38\text{ T}$ , line-averaged density  $2.0 \times 10^{13}\text{ cm}^{-3}$  and ECRH power  $P_{ECRH} = 380\text{ kW}$ . Strong burst of the soft X-ray oscillation can be observed during ECRH. The burst oscillations are located at the  $q = 1$  surface and its amplitude is clearly larger than that of the precursor oscillation. This mode is easier to distinguish from the precursor oscillation, because they not only appear before the sawtooth crash, but also in the middle of the sawtooth. The singular value

decomposition (SVD) analysis for the soft X-ray signals indicates the poloidal and toroidal mode number are  $m/n = 1/1$ . Figure 3 shows the temporal evolution of the hard X-ray photon number at different energy channels for the same shot. The energy distributions of the energetic electrons at the different time, expressed with the dot lines A, B, C and D in Fig.3 are show in Fig.4. Without ECRH, the energy distribution of the energetic electrons is Maxwell and the counts of the hard X-ray photons above 30keV are very low. During ECRH, the distributions deviate from Maxwell and the electrons with energy of 30-70keV increase obviously. Increasing level of the energetic electrons with more than 30keV strongly related with the burst of the soft X-ray oscillation, indicating that the internal kink mode surely is excited by energetic electrons. The e-fishbone not only can be excited during the off-axis ECRH deposited in high field side, but also in low field side.

The frequency of the mode is between 4 and 8 kHz. Fig.5 shows the time-frequency spectra obtained by wavelet analysis. It is found that the frequency decrease slightly with the decreasing of the amplitude of the burst. The frequency decrease may be related with the frequency chirping of the e-fishbone.

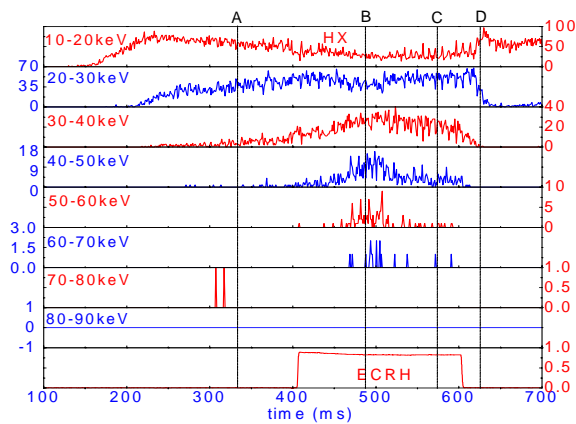


Fig.3. The temporal evolution of the hard X-ray photon number at different energy channels for shot 7982.

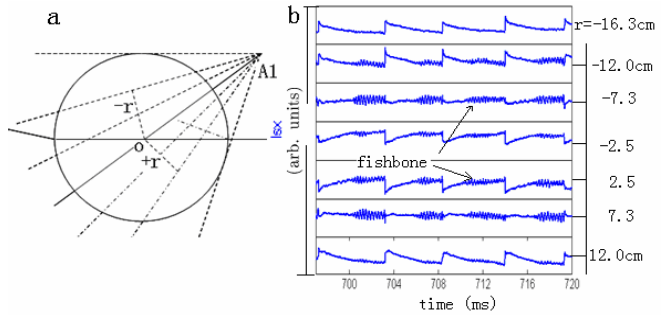


Fig.1. (a) The arrangement of a soft X-ray array (A1) on HL-2A; (b) The temporal evolution of the soft X-ray emission intensity at different channels for shot 4350.

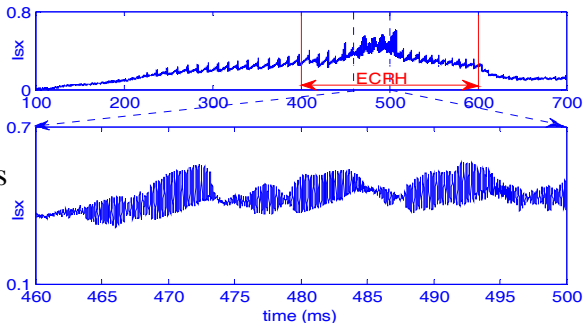


Fig.2. The temporal evolution of the soft X-ray emission intensity with e-fishbone for shot 7982.

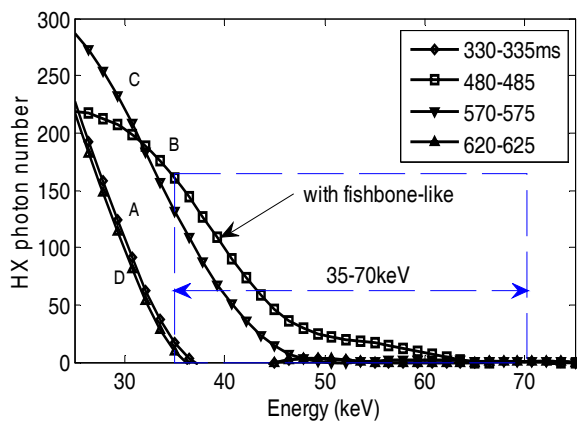


Fig.4. The hard X-ray photon numbers vs energetic electron energy at different time segments (A-D) for shot 7982.

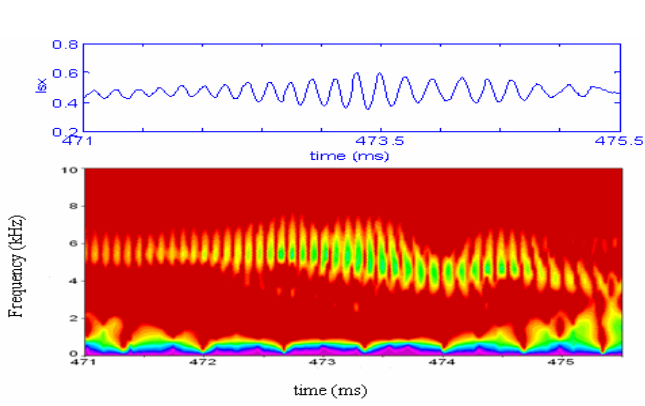


Fig.5. The soft X-ray signals with a “fishbone” and its time-frequency spectra.

The local soft X-ray emission is reconstructed by a tomographic technique, as shown in Fig.6. The ion diamagnetic drift velocity  $\vec{v}_{di} = \vec{B} \times \nabla p / enB^2$  is shown in Fig.6, where  $\nabla p$  is pressure gradient. The drift direction of the mode has been reconstructed by a tomographic technique, it is also presented in Fig.6, and it is clockwise direction. Namely, the mode propagates poloidally to parallel the electron diamagnetic drift velocity. The poloidal rotation of  $m = 1$  modes generally agrees in both sign and magnitude with the electron diamagnetic velocity.

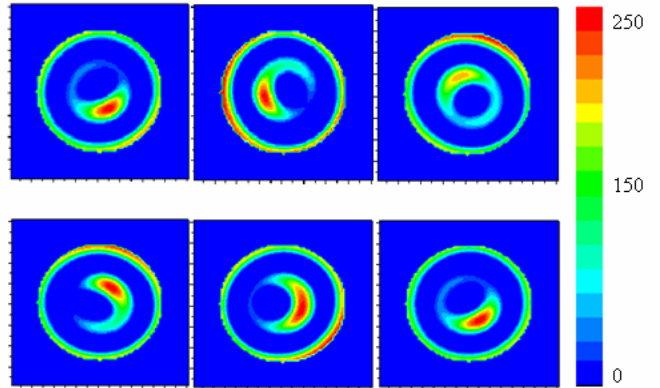
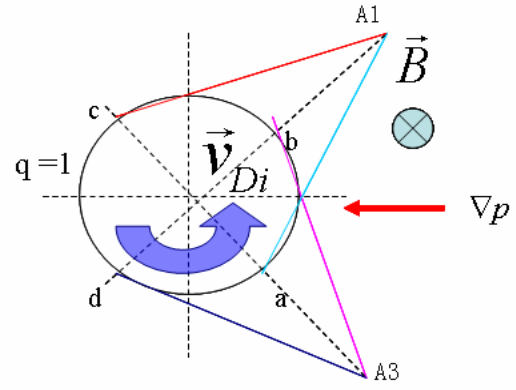


Fig.6. The direction of ion diamagnetic drift (A1 and A3 are two soft X-ray arrays) and the drift direction of the mode (reconstructed by a tomographic technique).

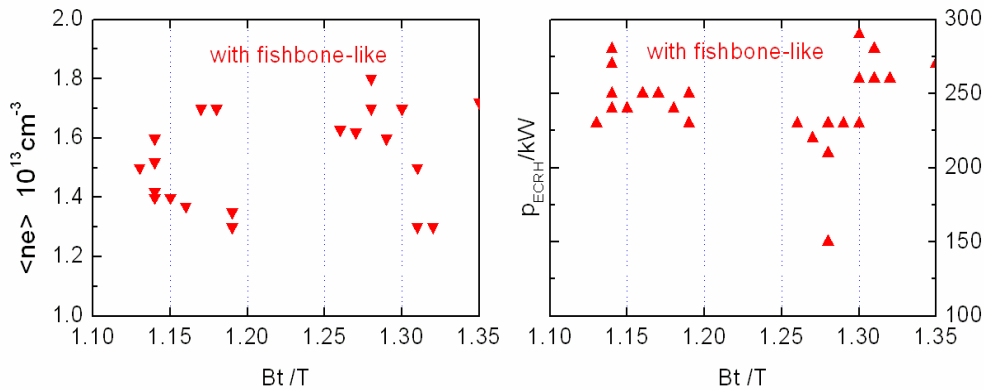


Fig.7. The toroidal field versus line-averaged density and ECRH power.

Since this phenomenon is related to the heating position, we have scanned the power deposited position from  $\rho = -0.4$  to  $0.4$  (namely toroidal magnetic field  $Bt$  from 1.10 to 1.35), where  $\rho$  is normalized radius (divertor discharges, minor radius  $a=37\text{cm}$ ). Fig.7 shows toroidal field  $Bt$  versus line-averaged density  $\langle ne \rangle$  and ECRH power  $P_{\text{ECRH}}$ . The heating position locates the LFS when  $Bt$  is larger than 1.21T, contrarily, lies in the HFS. It is found that this phenomenon could be observed on the HFS and LFS heating, and the

fishbone-like is excited much more easily during off-axis heating. For this reason, it is possible to produce easily a weak or negative magnetic shear with off-axis ECRH.

#### 4. Calculation and analysis

A general fishbone dispersion relation [12, 15-17] can be written as  $-i\Omega + \delta W_f + \delta W_k = 0$ , where  $\Omega = \omega^{1/2}(\omega - \omega_{*ip})^{1/2} / \omega_A$ ,  $\omega_{*ip}$  is the ion diamagnetic drift frequency,  $\omega_A = v_A / qR$ ,  $q$  is the safety factor,  $v_A$  is the Alfvén velocity. Here,  $-i\Omega$  is the inertial layer contribution due to energetic particles, while  $\delta W_f$  and  $\delta W_k$  come from fluid MHD and energetic particle contributions in the ideal regions.

The analysis of kinetic theory manifests four quantitatively different types of resonance between wave and energetic particles [15]. They are wave-precessional drift resonance ( $\omega = \omega_d$ ), wave-transit resonance ( $\omega = \omega_t$ ), wave-bounce resonance ( $\omega = \omega_b$ ) and precessional drift-bounce resonance ( $\omega_b \approx \omega_d \gg \omega$ ), where  $\omega_d$ ,  $\omega_b$ , and  $\omega_t \approx v_{\parallel} / qR$  are the toroidal precession frequency, the bounce frequency and the particle transit frequency around the torus, respectively.

The resonance conditions are different for trapped particles and circulating particles [18]. For the former, the resonance condition is  $\omega - \omega_d - p\omega_b = 0$ ; for the latter the resonance condition becomes  $\omega - k_{\parallel}v_{\parallel} - p\omega_t = 0$ .

The precession frequency  $\omega_{dt}$  and bounce frequency  $\omega_{bt}$  of the barely trapped electrons are given as follows [11, 18, 20]

$$\omega_{dt} = \frac{2\Omega_0 p_{\alpha}}{\gamma\Omega_p m_0 R^2} \left[ \frac{E(k_1)}{K(k_1)} - \frac{1}{2} \right] + \frac{4\Omega_0 p_{\alpha} s}{\gamma\Omega_p m_0 R^2} \left[ \frac{E(k_1)}{K(k_1)} - (1 - k_1^2) \right] = \frac{2\Omega_0 p_{\alpha}}{\gamma\Omega_p m_0 R_0^2} G_t, \quad \omega_{bt} = \frac{\pi(\varepsilon\Omega_0 p_{\alpha} / m_0)^{1/2}}{2\gamma q R_0 K(k_1)}$$

$$G_t = \frac{E(k_1)}{K(k_1)} - \frac{1}{2} + 2s \left[ \frac{E(k_1)}{K(k_1)} - (1 - k_1^2) \right], \quad k_1^2 = \frac{Rv_{\parallel}^2}{2r_s v_{\perp}^2}, \quad \cos\theta_b = 1 - 2k_1^2, \quad p_{\alpha} = \frac{1}{2} m_0 \Omega_c \rho^2$$

For the barely circulating electrons, the precession frequency  $\omega_{dc}$  and bounce frequency  $\omega_{bc}$  become [9, 14]

$$\omega_{dc} = q\omega_{bc} + \frac{u_{\phi_0}^2}{2\gamma\Omega_p r_s R_0} \left[ \frac{E(k)}{K(k)} - \left(1 - \frac{k^2}{2}\right) \right] + \frac{u_{\phi_0}^2 s}{\varepsilon\gamma\Omega_p R_0} \frac{E(k)}{K(k)} = q\omega_{bc} + \frac{u_{\phi_0}^2}{2\gamma\Omega_p r_s R_0} G_c$$

$$\omega_{bc} = \frac{\pi u_{\phi_0} \sigma}{2\gamma q R_0 K(k)}, \quad G_c = \frac{E(k)}{K(k)} - \left(1 - \frac{k^2}{2}\right) + 2s \frac{E(k)}{K(k)}, \quad k^2 = \frac{2r_s v_{\perp}^2}{Rv_{\parallel}^2}, \quad \sigma = \pm 1$$

where  $\Omega_0$ ,  $\Omega_p$  and  $\Omega_c$  are toroidal and poloidal gyro-frequency and guiding center gyro-frequency, respectively. Here we have used  $\gamma$ ,  $m_0$ ,  $s$ ,  $v_{\parallel}$ ,  $v_{\perp}$ ,  $r_s$ ,  $G$ ,  $\theta_b$ ,  $\varepsilon$ ,  $E$  and  $K$  to denote relativistic factor, static mass of electron, magnetic shear factor, parallel velocity, vertical velocity, reversal radius, normalized precession velocity, bounce angle of banana particles, inversed aspect ratio, the first and second complete elliptic integral, respectively.

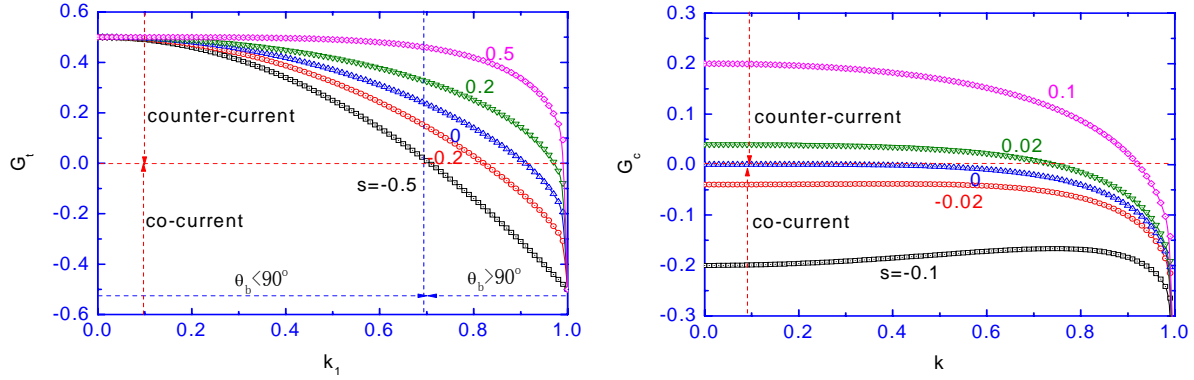


Fig.8. The normalized precession velocities ( $G_t$  and  $G_c$ ) of the barely trapped electrons and the barely circulating electrons. The negative values ( $G_t$  and  $G_c$ ) denote drift reversal for particles.

The normalized precession velocities ( $G_t$  and  $G_c$ ) of the barely trapped electrons and the barely circulating electrons have been present in Fig.8. For the trapped electrons, if the bounce angle  $\theta_b$  is larger than  $90^\circ$ , the precession velocity can reverse, and it easily take place in the region of negative shear. For the circulating electrons, the precession of all the particles is reversed if only the shear is negative.

Fig.9a shows the vertical energy of barely trapped electrons with precession frequency 5 kHz and  $Bt = 1.2$  T versus bounce angle. The e-fishbone can be excited if the bounce angle is larger than  $90^\circ$ , and it is more easily driven in the region of negative magnetic shear (-0.4, -0.2, -0.1 and -0.05) than

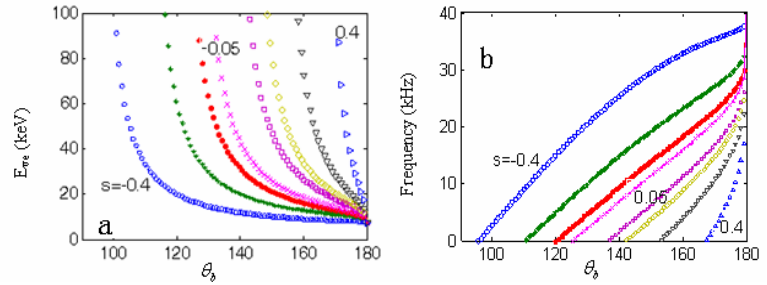


Fig.9. The vertical energy ( $E_{ve}$ ) and precession frequency of BTEs vs bounce angle  $\theta_b$  ( $s$  is magnetic shear)

that of positive magnetic shear (0.05, 0.1, 0.2 and 0.4). The vertical energy to resonate with internal kink mode is about 10-100 keV. The precession frequency of barely trapped electrons with vertical energy 60 keV and  $Bt = 1.2$  T versus bounce angle is plotted in Fig.9b, in which the precession frequency to resonate with internal kink mode ranges from 0 to 20 kHz ( $-0.2 \leq s \leq 0.2$  and  $90^\circ < \theta_b < 160^\circ$ ).

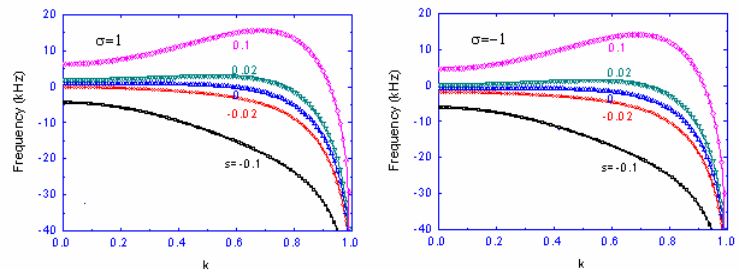


Fig.10. The precession frequency ( $\sigma = 1$  and  $\sigma = -1$ ) of BCEs vs  $k$  at parallel energy  $E_p = 40\text{keV}$ . The negative frequencies denote drift reversal for circulating particles.

Fig.10 gives the precession frequency of barely

circulating electrons with parallel energy  $E_p = 40$  keV and  $B_t = 1.2$  T versus  $k$ . The precession frequency to resonate with internal kink mode is in the range of 0-20 kHz ( $-0.1 \leq s \leq 0$  and  $k < 0.8$ ).

## 5. Summary

The experimental phenomena associated with the e-fishbone are summarized as follows: (1) It has been experimentally identified that the energetic electrons, which deviate from Maxwell velocity distribution, interact with internal kink mode; (2) The structure of the e-fishbone is located at the  $q = 1$  flux surface and the e-fishbone can be excited by ECRH deposited on both the LFS and HFS, and the mode occurs much more easily during off-axis heating; (3) The mode has a bursting behavior, and the frequencies of the mode are between 4 and 8 kHz; (4) The modes propagate toroidally parallel to the precession velocity of deeply trapped ions which is in the same direction as the plasma current, and propagate poloidally parallel to the electron diamagnetic drift velocity.

It is experimentally identified that the energetic electrons with energy of 35-70 keV play a dominant role in the excitation mechanism of the e-fishbone. By the wave-particle resonance conditions, the calculation analyses show that the mode frequency is close to the precession frequency of the BTEs and BCEs when the magnetic shear is very weak or negative, in accordance with experiment observations. The e-fishbone is supposed to be excited by the BCEs with off-axis ECRH on the LFS. However, on the HFS, the mode is likely to be driven jointly by the BTEs and BCEs.

Using CdTe detectors, the energy spectrum of the energetic electron can be obtained, but we cannot differentiate the perpendicular and parallel energy of energetic electrons. Strictly speaking, a quantitative analysis of the e-fishbone needs a three-dimensional Fokker-Planck simulation which we intend to pursue in the future. Theoretically, both the BTEs and BCEs can be characterized by drift-reversal and can excite e-fishbone propagating in the ion diamagnetic direction or electron diamagnetic direction; for all that, this still requires much more experimental evidences.

## Acknowledgments

The authors would like to acknowledge Dr G.Y. Fu for helpful discussions during attending SU-HANG meeting and thank Professor X.M.Qiu, J.Q.Dong, and Z.T.Wang for helpful advice and assistance on physical analysis. This work was supported by National Natural Science Foundation of China under Grant No. 10775041.

## References

- [1] Fasoli A *et al* **2007** *Nucl. Fusion* **47** S264-S284
- [2] McGuire K *et al* **1983** *Phys.Rev.Lett.* **50** 891
- [3] Gunter S *et al* **1999** *Nucl. Fusion* **39** 1535-1539
- [4] Fredrickson E *et al* **2003** *Nucl. Fusion* **43** 1258-1264

- [5] Wong K L *et al* **2000** *Phys. Rev. Lett.* **85** 996
- [6] Ding X T *et al* **2002** *Nucl. Fusion* **42** 491
- [7] Yan L W *et al* **2001** *Chin. Phys. Lett.* **18** 1227
- [8] Smeulders P *et al* **2002** 29th EPS Conf. on Contr. Fusion and Plasma Phys. ECA Vol. **26B** D-5.016
- [9] Zonca F *et al* **2007** *Nucl. Fusion* **47** 1588
- [10] Maget P *et al* **2006** *Nucl. Fusion* **46** 797
- [11] Wang Z T *et al* **2006** *Chin. Phys. Lett.* **23** 158
- [12] Chen L *et al* **1984** *Phys. Rev. Lett.* **52** 1122
- [13] Coppi B and Porceli F **1986** *Phys. Rev. Lett.* **57** 2272
- [14] Wang Z T *et al* **2007** *Nucl. Fusion* **47** 1307
- [15] Tsai S T and Chen L **1993** *Phys. Fluids B* **5** 3284
- [16] Wesson J **2004** *Tokamaks* (Oxford: Oxford University Press) 400
- [17] Biglari H and Chen L **1991** *Phys. Rev. Lett.* **67** 3681
- [18] Chen L and Zonca F **2007** *Nucl. Fusion* **47** S727
- [19] Hazeltine *et al* **1972** *Phys. Fluids* **24** 1164
- [20] Connor J W *et al* **1983** *Nucl. Fusion* **23** 1702